DIFFRACTION MODELING FOR INTERACTIVE VIRTUAL ACOUSTICAL ENVIRONMENTS

Bill Kapralos
Faculty of Business and Information Technology, University of Ontario Institute of Technology
200 Simcoe Street North, Oshawa, Ontario, Canada. L1H 7K4.
bill.kapralos@uoit.ca

Michael Jenkin
Dept. of Computer Science and Engineering, Centre for Vision Research, York University. Toronto, Ontario, Canada. M3J 1P3.
jenkin@cse.yorku.ca

Evangelos Milios
Faculty of Computer Science, Dalhousie University. Halifax, Nova Scotia, Canada. B3H 1W5.
eem@cs.dal.ca

Keywords: Sonel mapping, acoustical diffraction modeling, virtual environments

Abstract: Since the dimensions of many of the objects/surfaces encountered in our daily lives are within an order of magnitude of the wavelength of audible sounds, diffraction is an elementary means of sound propagation. Despite its importance in the real-world, diffraction effects are often overlooked by acoustical modeling methods leading to a degredation in immersion or presence. This paper describes an acoustical diffraction method based on the Huygens-Fresnel principle. The method is simple and efficient allowing it to be incorporated in interactive acoustical environments including virtual environments. Experimental results are presented that illustrate the performance and effectiveness of the method and its conformance to theoretical diffraction models.

1 INTRODUCTION

Diffraction refers to the "bending mode" of sound propagation whereby sound waves go ("bend") around an obstacle that lies directly in the line of straight propagation between the sound source and receiver. Diffraction is dependent on both wavelength and obstacle/surface size, increasing as the ratio between wavelength and obstacle size is increased (Cremer and Müller, 1978). Since the dimensions of many of the objects/surfaces encountered in our daily lives are within an order of magnitude as the wavelength of audible sounds, diffraction is an elementary means of sound propagation, especially when there is no direct path between the sound source and the receiver (Tsingos et al., 2002).

Diffraction is a phenomenon of all wave propagation including sound and light waves and several approaches have been developed to model its effects. One such approach is the Huygens-Fresnel principle, originally formulated by Christian Huygens in 1678 and later modified and extended by Augustin Fresnel. Although it is a rather simple approach, it can satisfactorily model a large number of diffraction configurations in a simple and efficient manner. The Huygens-Fresnel principle is based on the assumption that at every time instant, every point on a primary wavefront of an emitted sound can be thought of as a continuous emitter of secondary wavelets (sources) and these secondary wavelets combine to produce a new wavefront in the direction of propagation. This assumption fits nicely with particle-based acoustical modeling methods whereby the acoustics of an environment is determined by emitting sound "particles" from a sound source and tracing them through the environment. One such particle-based method is *sonel mapping* (Anonymous, 2006). Sonel mapping is a two-pass probabilistic, "particle-based", acoustical modeling method inspired by the popular image synthesis photon mapping method (Jensen, 2001). Sonel mapping models the propagation of sound within an environment, taking into account the relevant acoustical phenomena experienced by a propagating sound in an efficient manner for use in dynamic virtual environments. This paper describes an efficient acoustical diffraction modeling technique based on the Huygens-Fresnel principle. The technique described is incorporated within the sonel mapping method although it could easily be incorporated into other geometric-based acoustical modeling methods.

The remainder of this paper is organized as follows. Section 2 reviews several available acoustical diffraction methods for virtual environment ap-

plications. Section 3 provides a brief introduction to the optics-based Huygens-Fresnel principle followed by a detailed description of the acoustical diffraction method. Section 4 provides the results of experiments conducted to demonstrate the effectiveness of the developed acoustical diffraction modeling method. Finally, concluding remarks are given in Section 5.

2 BACKGROUND

The two major approaches to computational acoustical modeling (e.g., estimating the room impulse response) are (Funkhouser et al., 2004) *wave-based modeling* whereby numerical solutions to the wave equation are sought and *geometric modeling* whereby sound is approximated as a ray phenomenon and traced through the scene. Although wave-based methods can account for non-specular reflection phenomena, they are very expensive computationally making them impractical for all but very simple, static environments. Geometric modeling, and in particular ray-based approaches are the most widely used due to their simplicity and computational feasibility. Geometric modeling methods such as *image sources* (Allen and Berkley, 1979) and *ray tracing* (Krokstad et al., 1968; Kulowski, 1985) assume that sound is a ray phenomena (Cremer and Müller, 1978) and model all interactions between sound rays and objects/surfaces as specular. As a result, they typically ignore the wavelength of sound and any phenomena associated with it including diffraction (Calamia et al., 2005).

That being said, a limited number of research efforts have investigated acoustical diffraction modeling. The beam tracing approach of Funkhouser *et al.* (2003) for acoustical modeling/rendering includes an extension capable of approximating diffraction. Their frequency domain method is based on the *uniform theory of diffraction* (UTD) (Keller, 1962). Validation of their approach by Tsingos *et al.* (2002) involved a comparison between actual impulse responses (e.g., the energy reaching a receiver over a period of time) measured in a simple enclosure (the "Bell Labs Box") and the impulse responses obtained by simulating the enclosure. Tsingos *et al.* (2002) observed that their combined technique was the first instance to use a physically-based diffraction model to produce interactive rate sounds in a complex virtual environment.

Tsingos and Gascuel (1997) developed an occlusion and diffraction method that utilizes computer graphics hardware to perform fast sound visibility calculations that can account for specular reflections, absorption, and diffraction caused by partial occluders. Diffraction is approximated by computing the fraction of sound that is blocked by obstacles (occluders) between the path from the sound source to the receiver by considering the amount of volume of the first Fresnel ellipsoid blocked by the occluders. Rendering of occluders is performed from the receiver's position. A count of all pixels not in the background is taken and pixels that are "set" (e.g., not in the background) correspond to occluders. Their approach is near-real-time using graphics hardware to operate in an efficient manner.

In later work, Tsingos and Gascuel (1998) introduced another occlusion and diffraction method based on the Fresnel-Kirchoff optics-based approximation to diffraction. As with the Huygens-Fresnel approximation, the Fresnel-Kirchoff approximation is based on Huygens' principle. The total unoccluded sound pressure level at some point p in space is determined by calculating the sound pressure of a small differential area dS and integrating over the closed surface enclosing p. After determining the total unoccluded sound arriving at point p from a sound source, diffraction and occlusion effects are accounted for by computing an *occlusion depth-map* of the environment between the sound source and the receiver (listener) using computer graphics hardware to permit real-time operation. Once this depth-map has been computed, the depth of any occluders between the sound source and the receiver can be obtained from the Z-buffer whereby "lit" pixels correspond to occluded areas. The diffraction integral described by the Fresnel-Kirchoff approximation is then approximated as a discrete sum of differential terms for every occluded pixel in the Z-buffer. Comparisons for several configurations with obstacles of infinite extent made between their method and between boundary element methods (BEMs), produced "satisfactory quantitative results" (Tsingos and Gascuel, 1998).

3 DIFFRACTION MODELING

The Huygens-Fresnel principle states that every point on the primary wavefront can be thought of as a continuous, direction dependent emitter of secondary wavelets (sources) that combine to produce a new wavefront in the direction of propagation (Hecht, 2002). These secondary wavelets are emitted in a direction dependent manner, essentially scaled by an *obliquity* or *inclination* factor $K(\theta)$ as

$$K(\theta) = \frac{1}{2}(1+\cos(\theta)) \tag{1}$$

where θ is the angle between the receiver and the direction of propagation of the primary wavefront (Hecht, 2002). This expanding wavefront can be divided into a number of ring-like regions, collectively

known as *Fresnel zones* (Hecht, 2002). The boundary of the i^{th} Fresnel zone (Z_i) corresponds to the intersection of the wavefront with a sphere of radius $r_\circ + i\lambda/2$ centered at the receiver where, $r_\circ$ is equal to the distance between the receiver and the expanding wavefront after it has traversed a distance of ρ from the sound source. In other words, the distance from the receiver to each adjacent Fresnel zone differs by half a wavelength ($\lambda/2$). Each Fresnel zone contains secondary sources that are assumed to emit their energy in phase with the primary wave. The secondary sources within each Fresnel zone i emits energy collectively equal to E_i and a portion of this energy may reach the receiver. By summing the contribution of energy reaching the receiver from each of the Fresnel zones, the total energy leaving the sound source and reaching the receiver (E_{total}) can be calculated. It can be shown that the total energy is approximately equal to half the energy of the first Fresnel zone reaching the receiver (Hecht, 2002) or, mathematically $E_{total} \approx |E_1|/2$. A detailed mathematical derivation of the Huygens-Fresnel principle is presented by Hecht (2002).

3.1 Huygens-Fresnel Acoustical Diffraction Modeling

In the sonel mapping method (Anonymous, 2006), at each sound source, sonels are emitted and traced through the environment while recording their interaction with any surfaces/objects they may encounter. Upon encountering a surface, a decision is made as to whether the sound particle (known as a *sonel*) will be reflected specularly or diffusely, diffracted or completely absorbed (the decision is made probabilistically based on various parameters including frequency, distance to an edge, etc. using a Russian roulette strategy (Kapralos et al., 2005)). Whether or not the sonel is actually incident on the edge itself or close to the edge, if the sonel is to be diffracted, its position is assumed to be on the edge (p_{edge}). Since the position of both the sound source and p_{edge} are known, the distance between them r_{se} can be determined. The radius of the primary wavefront is then set to this distance (e.g., $\rho = r_{se}$ - see Figure 1).

Since ρ is the distance between the position of the sound source and p_{edge}, p_{edge} must be located on the surface of the wavefront and within one of the Fresnel zones (the "initial" Fresnel zone) denoted by Z_{init} and calculated as

$$Z_{init} = \left\lfloor \frac{r_{init} - r_\circ}{\lambda} + 0.5 \right\rfloor. \quad (2)$$

Here r_{init} is the distance between the receiver and p_{edge} and $r_\circ$ is the distance between the receiver and

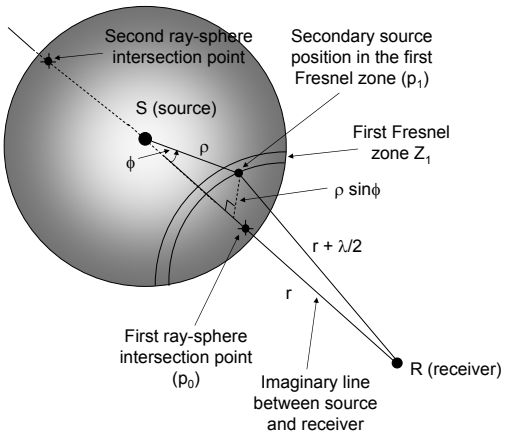

Figure 1: Determining the position of a secondary source within the first Fresnel zone.

primary wavefront given as $r_\circ = r_{SR} - \rho$ where, r_{SR} is the distance between the sound source and the receiver. Although p_{edge} may lie anywhere within Z_{init} and not necessarily on its boundary, it is assumed that the obliquity factor is constant throughout the entire zone (Hecht, 2002) and therefore, its position within the zone does not matter. Given the position of the secondary source in Z_{init}, the position of a secondary source within the first Fresnel zone (Z_1) can be determined. Referring to Figures 1 and 2, this is accomplished in two steps:

1. Rotate p_{edge} such that it lies directly on the (imaginary) line between the sound source and receiver. This essentially moves p_{edge} to a new position denoted by $p_\circ$.
2. Move $p_\circ$ to yet another new position (p_1) within the first Fresnel zone.

Determining $p_\circ$***:*** The original position p_{edge} that lies within Z_{init} is rotated such that it lies directly on the (imaginary) line between the sound source and receiver. This can be performed using a series of rotations about the central axes. However, this is actually accomplished by taking the (first) point of intersection (denoted by $p_\circ$) between the sphere representing the initial wavefront and a ray (normalized vector) whose origin is the receiver position and whose direction is towards the sound source.

Determining p_1***:*** Once the intersection point ($p_\circ$) has been determined, it is moved to the first Fresnel zone. Referring to Figures 1 and 2, angles θ (the horizontal angle of $p_\circ$ relative to the sound source) and ϕ (the vertical angle of $p_\circ$ relative to the sound source) are calculated as

$$\theta = tan^{-1}\left(\frac{x_p - x_s}{z_p - z_s}\right), \quad \phi = cos^{-1}\left(\frac{y_p - y_s}{\rho}\right) \quad (3)$$

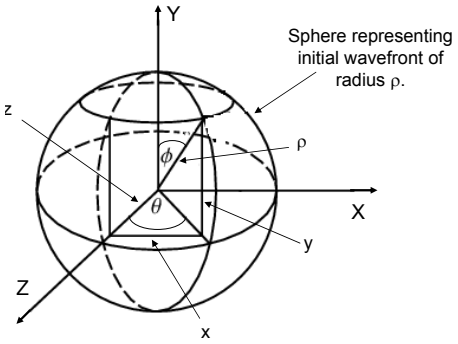

Figure 2: Spherical coordinates.

where (x_s, y_s, z_s) and (x_p, y_p, z_p) are the spatial coordinates of the sound source and $p_\circ$ respectively. As with $p_\circ$, the position of the secondary source in the first Fresnel zone (p_1) also lies on the surface of the sphere corresponding to the initial propagating wavefront of radius ρ. The difference in distance between adjacent Fresnel zones and the receiver is $\lambda/2$. Therefore, the difference in distance (r_{diff}) between the receiver and $p_\circ$ and the receiver and the secondary source in the first Fresnel zone p_1 must also be $\lambda/2$. Position p_1 is determined iteratively until r_{diff} is within ε of $\lambda/2$. Once the position of a secondary source within the first Fresnel zone (Z_1) has been determined, the energy (E_1) reaching the receiver from Z_1 can be calculated as (Hecht, 2002)

$$\begin{aligned} E_1 &= (-1)^{1+1}\frac{2K_1(\theta)E_A\rho\lambda}{(\rho+r_\circ)}\sin[\omega t - k(\rho+r_\circ)] \\ &= \frac{2K_1(\theta)E_A\rho\lambda}{(\rho+r_\circ)}\sin[\omega t - k(\rho+r_\circ)]. \end{aligned} \quad (4)$$

Here $K_1(\theta)$ is the obliquity factor of Z_1 and $r_\circ$ is the distance between the receiver and the expanding wavefront after it has traversed a distance of ρ from the sound source. t is the time taken for a secondary source in Z_1 to reach the receiver, $k = 2\pi\lambda$ is the wavenumber and E_A is the energy per unit area of the secondary sources within a differential area of the Fresnel zone (see (Hecht, 2002)). Adding terms to account for absorption of sound energy by the medium (air), Equation 4 becomes

$$E_1 = K_1(\theta)\times E_\circ e^{-m(\rho+r_\circ)}\times\sin[\omega t - k(\rho+r_\circ)] \quad (5)$$

where $E_\circ$ is the ray energy and m is the air absorption constant that varies as a function of the conditions of the air itself. As presented above, the energy reaching the receiver from the first Fresnel zone can be calculated assuming an obstruction-free path between each zone and the receiver (e.g., the first zone is completely visible to the receiver). Edge effects are accounted for by considering the *visibility weighting* v_1 for the first zone Z_1 relative to the receiver using ray casting. n_{rays} rays are emitted from the receiver to uniformly sampled positions within Z_1. A check is made to determine whether each sampled position is visible relative to the receiver (see Figure 3). The visibility weighting is determined by considering the number of visible (non-blocked) rays (n_{vis}) relative to the total number of emitted rays (N_{vis}) or, mathematically, $v_1 = n_{vis}/N_{vis}$. Taking edge effects into account, the total energy reaching the receiver from the first Fresnel zone Z_1 is given as

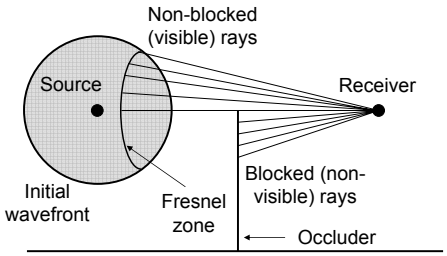

Figure 3: Sampling a Fresnel zone in the presence of an occluding edge using ray-casting.

$$E_1 = v_1\times K_1(\theta)\times E_\circ e^{-m(\rho+r_\circ)}\times\sin[\omega t_1 - k(\rho+r_\circ)] \quad (6)$$

where $t_1 = (r_\circ + \lambda/2)/v_s$ is the time taken for the secondary sources within the first Fresnel zone to reach the receiver and $v_s = 343m\cdot s^{-1}$ is the speed of sound in air.

3.2 Considering All Fresnel Zones

Rather than considering the first Fresnel zone only, the entire sphere representing the initial wavefront emitted from the sound source is divided into different Fresnel zones. The energy arriving at the receiver from each of these Fresnel zones is summed to determine the amount of energy reaching the receiver. The total number of zones (N_{zones}) is given by

$$N_{zones} = \left\lfloor \frac{2\rho}{(\lambda/2)} \right\rfloor. \quad (7)$$

To account for diffraction effects, a visibility factor for each Fresnel zone is introduced. The visibility factor (denoted by v_i), represents that fraction of the i^{th} Fresnel zone visible relative to the receiver. As with the first zone-only approximation previously described, the edge position p_{edge} is assumed to lie on the sphere representing the initial wavefront and within a particular Fresnel zone Z_{init}. Given the position of the secondary source in Z_{init}, the position of a secondary source within the first Fresnel zone (p_1) can be determined using the two step process previously described. Upon determining p_1, simple geometry allows for the position of a secondary source within Fresnel zone Z_2 to be determined. The same reasoning can be applied to finding the position of a

secondary source within the third Fresnel zone and subsequent zones until the position of a secondary source within all the Fresnel zones considered has been found (the mathematics describing this process are developed in Section 3.2.1). Once the position of a secondary source within a zone Z_i has been determined, the energy reaching the receiver from Z_i can be calculated using Equation 5.

Edge effects are accounted for by considering the visibility weighting v_i of each zone Z_i relative to the receiver, using ray casting as described in the previous section. Taking edge effects into account, the total energy reaching the receiver from zone Z_i is given as

$$E_i = v_i \times (-1)^{i+1} \times K_i(\theta) \times E_\circ e^{-m(\rho+r_\circ)} \times \sin[\omega t_i - k(\rho+r_\circ)] \quad (8)$$

where $t_i = (r_\circ + i\lambda/2)/v_s$ is the time taken for the secondary sources within Fresnel zone i to reach the receiver. The total energy E_{total} reaching the receiver from the sound source taking edge effects into consideration is determined by summing the energy reaching the receiver from each of the N Fresnel zones

$$E_{total} = (v_1 \times E_1) + (v_2 \times E_2) + \cdots + (v_N \times E_N). \quad (9)$$

3.2.1 Finding the Position of a Secondary Source Within a Fresnel Zone

The distance between secondary sources in adjacent zones (e.g., between zones Z_1 and Z_2) is $\lambda/2$. Referring to Figure 1

$$dS = \rho d\varphi 2\pi(\rho \sin\varphi). \quad (10)$$

Applying the law of cosines,

$$r^2 = \rho^2 + (\rho + r_0)^2 - 2\rho(\rho + r_0)\cos\varphi \quad (11)$$

where r is the distance between the receiver and the secondary source in a particular Fresnel zone. By rearranging Equation 11, an expression for ϕ, the angle between the line connecting the sound source and receiver and the line from the sound source to the secondary source, can be determined

$$cos\phi = \frac{r^2 - \rho^2 + (\rho + r_\circ)^2}{-2\rho(\rho + r_\circ)}. \quad (12)$$

By differentiating Equation 11 above, an expression for the value of $2rdr$ can be obtained (e.g., $2rdr = 2\rho(\rho + r_\circ)\sin(\varphi)d\varphi$) where dr is the difference in distance between the receiver and the secondary sources between adjacent differential areas dS. Since a particular Fresnel zone is comprised of several differential areas, the value of dr is not necessarily equal to $\lambda/2$. Here dr is set to a value of $\lambda/2$ thus representing an adjacent Fresnel zone as opposed to an adjacent differential area within a zone. With the values of both dr and ϕ, an expression for $d\phi$ is obtained

$$d\phi = \frac{2rdr}{2\rho(\rho + r_\circ)sin\phi}. \quad (13)$$

Referring to Figure 1, since the elevation angle θ and the radius of the initial wavefront ρ remain constant the position of a secondary source in the adjacent zone can now be determined. This is accomplished by solving for each of its x,y,z coordinates using the equations for the Cartesian coordinates (see Figure 2) of the sphere along with the previously computed value of $d\phi$

$$x = x_s + (\rho sin(\theta)sin(\phi + d\phi)) \quad (14)$$

$$y = y_s + (\rho sin(\theta)cos(\phi + d\phi)) \quad (15)$$

$$z = z_s + (\rho cos(\theta)). \quad (16)$$

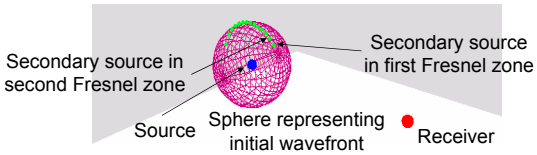

Figure 4: Sampling a secondary source within a particular Fresnel zone considering a 63Hz sound source.

Figure 4 provides a graphical illustration of the sampling of a secondary source in each Fresnel zones for a 63Hz sound source.

4 EXPERIMENTAL VALIDATION

A series of experiments are presented that describe the effectiveness of the developed acoustical diffraction modeling method.

4.1 Model Correctness

In this experiment the validity of the energy reaching a receiver as calculated using the Huygens-Fresnel principle is examined. This is accomplished by considering the energy reaching the receiver from the sound source using both Huygens-Fresnel implementations (one Fresnel zone only and all Fresnel zones) with the visibility of the first Fresnel zone assumed to be one and comparing the results with the results obtained using the harmonic spherical wave model (Hecht, 2002)

$$E = \frac{E_\circ}{\rho} cos(\omega t' - k\rho). \quad (17)$$

Here, E is the energy arriving at the receiver $E_\circ$ is the energy of the source at time $t = 0$. ρ is the radius of the sphere representing the initial wavefront

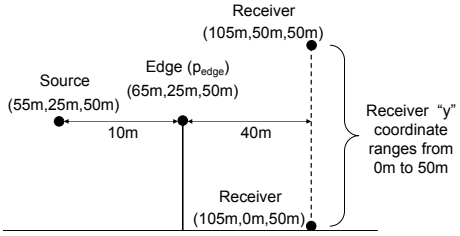

Figure 5: Room set-up used in the correctness of the acoustical diffraction method simulation.

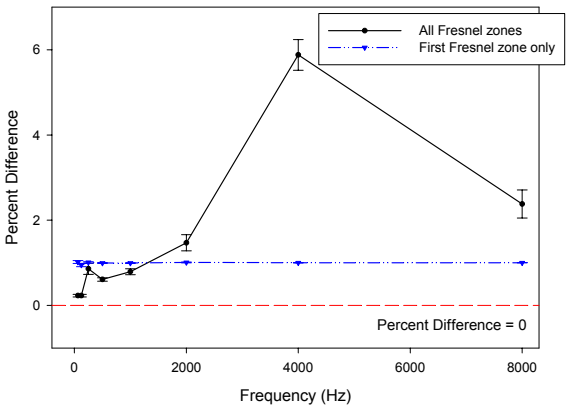

Figure 6: Graphical summary of the results for the correctness of the acoustical diffraction method simulation. Average percentage difference between the energy as simulated using both Huygens-Fresnel implementations and the energy as calculated with the harmonical spherical wave model averaged over all 51 positions for each frequency) along with error bars (standard deviation) as a function of frequency.

and set to a value equal to the distance between the sound source and the position on the edge (P_{edge}). t' is the time it takes for the wave to propagate a distance ρ (e.g., $t' = \rho/343m \cdot s^{-1}$). As shown in Figure 5, the sound source and edge position (p_{edge}) remained stationary while the receiver's position (the "y" coordinate) was varied in unit increments from $y = 0$m to $y = 50$m. The experiment considered the following frequencies: 63Hz, 125Hz, 250Hz, 500Hz, 1kHz, 2kHz, 4kHz and 8kHz. The experiment was repeated using the acoustical diffraction models where only the first Fresnel zone was considered and where all Fresnel zones were considered. A graphical summary of the results is presented in Figure 6 where the average percentage difference (e.g., the difference between the energy as simulated using sonel mapping and the energy as calculated with the harmonical spherical wave model averaged over all 51 positions for each frequency) is plotted against frequency for each of the two scenarios considered. The smallest and largest average percentage difference for the diffraction implementation whereby only the first Fresnel zone was considered are small, 0.99 and 1.02 respectively. Despite ignoring the energy of all zones other than the first, this implementation provides a reasonable approximation. In contrast, the range of percentage differences for the diffraction implementation where all Fresnel zones were considered is larger, ranging from 0.23 to 5.88 and typically increase with increasing frequency. This increase in percentage difference may be due to numerical errors associated with locating a secondary source in each of the Fresnel zones. As frequency increases, the number of Fresnel zones also increases thus, any errors associated with locating a secondary source in a particular Fresnel zone propagates through (e.g., locating a secondary source in Fresnel zone i requires the position of a secondary source in zone $i-1$). Therefore, an error in the position of the secondary source in zone $i-1$ may propagate and therefore, result in an incorrect secondary source position in zone i.

4.2 First Fresnel Zone Visibility as a Function of Receiver Height

In this simulation, the visibility of the first Fresnel zone relative to the receiver and the sound level at the receiver was examined as a function of frequency. A stationary sound source was positioned at coordinates (40m, 25m, 50m) and the edge position (p_{edge}) was set at coordinates (50m, 25m, 50m). The receiver was positioned at three locations: i) below the edge position at coordinates (110m, 24m, 50m) (Figure 7(a)), ii) at the same height as the edge position at coordinates (110m, 25m, 50m) (Figure 7(b)), and iii) above the edge position at coordinates (110m, 26m, 50m) (Figure 7(c)). For each of the three scenarios, the energy reaching the receiver was calculated for each of the following frequencies: 63Hz, 125Hz, 250Hz, 500Hz, 1000Hz, 2000Hz, 4000Hz and 8000Hz. Frequency dependent attenuation of the sound by the air was ignored to allow for the frequency dependent diffraction effects to be examined. The purpose of this experiment is to compare the Huygens-Fresnel diffraction implementation with the theoretical diffraction model that states diffraction increases with increasing frequency (decreasing wavelength) for various sound source, edge and receiver configurations. Since the visibility of the first Fresnel zone is directly related to the amount of energy reaching the receiver via diffraction, frequency vs. visibility is used as a measure of performance. A graphical summary of the results for each of the three scenarios is provided in Figures 8. In Figure 8(a), the visibility of the first Fresnel zone relative to the receiver is plotted as a function of frequency. In Figure 8(b), receiver level

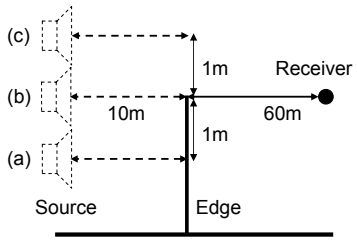

Figure 7: Set-up for the first Fresnel zone visibility as a function of receiver height simulation. With respect to the y-axis, receiver is: (a) below the edge position, (b) at same height as the edge position and (c) above the edge position.

is plotted as a function of frequency. In both plots, the filled circles and solid line represents the first scenario where the receiver is below the edge position. The open circle and short dashed line represents the scenario where the receiver is at the same height as the edge position (and above the sound source) and the triangle and long dashed line represents the scenario where the receiver is above the edge position. The results for the configuration considered in the first scenario (e.g., receiver below the edge position) are as expected. In particular, the visibility of the first Fresnel zone is inversely proportional to frequency whereby, as frequency increases, visibility decreases. The decrease in visibility is due to a decrease in the size of the first Fresnel zone and this results in a decrease in the sound energy reaching the receiver. As a result, as frequency increases, the sound energy reaching the receiver decreases, thus conforming to the theoretical model that predicts an increase in diffraction as frequency decreases (Cremer and Müller, 1978). In particular, the visibility of the first Fresnel zone is used to scale the unoccluded energy reaching the receiver after being emitted from the sound source. Since there is a direct relationship between visibility and energy reaching the receiver (e.g., as visibility increases, the energy reaching the receiver increases as well), visibility will increase with increasing frequency.

The results of the second scenario where the receiver was positioned at the same height as the edge position are also as expected. The visibility is approximately 0.5 irrespective of frequency indicating that half of the zone is visible relative to the receiver. Finally, in the third scenario where the height of the receiver is greater than the height of the edge, visibility and frequency share a direct relationship whereby visibility increases with increasing frequency. This is due to the fact that as frequency increases, Fresnel zone size decreases and therefore, when the height of the receiver is greater than the height of the edge, less of the Fresnel zone will be occluded.

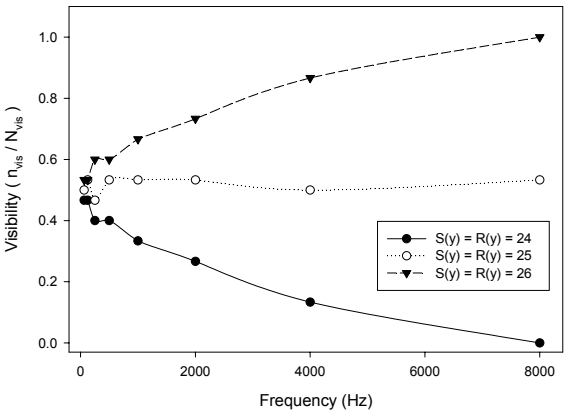

(a) Frequency vs. visibility.

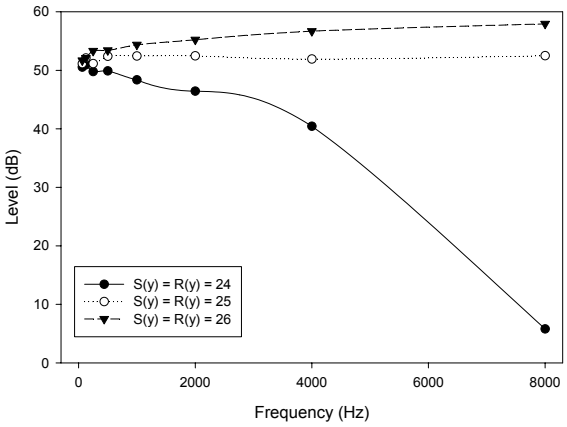

(b) Frequency vs. level

Figure 8: Results for the first Fresnel zone visibility as a function of receiver height simulation: frequency vs. visibility and sound level for various sound source and receiver heights relative to the edge position. (a) Frequency vs. visibility and (b) frequency vs. receiver sound level.

4.3 Running Time Requirements

This simulation examines the running time requirements of the Huygens-Fresnel acoustical diffraction modeling approach. Both implementations (first Fresnel zone only and all Fresnel zones) were considered. The simulation was performed for the configuration of the previous experiment. The sound source and edge position (p_{edge}) were constant at positions (65m, 80m, 80m) and (85m, 82m, 85m) respectively while the receiver position varied across the y and z coordinates (e.g., a plane of receiver positions with y and z beginning at position (85m, 75m, 75m) and ending at position (85m, 85m, 85m)). The results of this simulation are summarized in Figure 9 where the average running time and standard deviation for each frequency band (obtained over 225 measurements) to compute the diffraction modeling are given. When considering the first Fresnel zone only, the difference

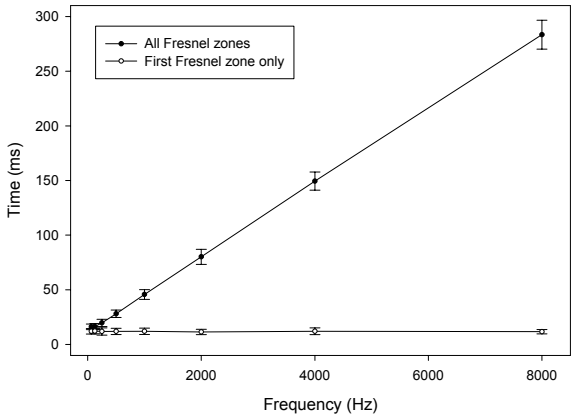

Figure 9: Results for the diffraction running time requirements simulation: average diffraction modeling running time vs. frequency with error bars (standard deviation).

in running time from the smallest (11.42ms for the 200Hz center frequency) to the largest running time (12.27ms for the 125Hz center frequency) is 0.85ms and therefore, running time is approximately constant across frequency. In contrast, the running time when considering all Fresnel zones increases linearly with frequency, ranging from 16.90ms (63Hz) to 283.42ms (8000Hz). In addition to the first Fresnel zone only implementation providing more accurate results (as demonstrated in the simulation described in Section 4.1), its running time requirements are much less and constant across frequency. This is of course directly related to the additional time required to determine the position of a secondary source in each additional Fresnel zone in addition to calculating the visibility weighting of each additional Fresnel zone relative to the receiver.

5 CONCLUSIONS

This paper presented a simple method capable of modeling acoustical edge diffraction effects in an efficient manner. The method is inspired by the Huygens-Fresnel principle which assumes a propagating wavefront is composed of a number of secondary sources. This fits nicely within particle-based (geometric) acoustical modeling methods such as sonel mapping whereby acoustical wave propagation is approximated by propagating sound particles (sonels) from a sound source and tracing them through the environment. Experimental results demonstrate that diffraction effects can be approximated in a very simple and efficient manner allowing computation at interactive rates. Although the Huygens-Fresnel principle is a rather simple approach, it can satisfactorily describe a large number of diffraction configurations in an efficient manner.

REFERENCES

Allen, J. B. and Berkley, D. A. (1979). Image method for efficiently simulating small-room acoustics. *Journal of the Acoustical Society of America*, 65(4):943–950.

Anonymous (2006). Sonel mapping: A stochastic acoustical modeling system. In *Proc. IEEE International Conference on Acoustics, Speech and Signal Processing*, Toulouse, France.

Calamia, P. T., Svensson, U. P., and Funkhouser, T. A. (2005). Integration of edge-diffraction calculations and geometrical-acoustics modeling. In *Proceedings of Forum Acusticum 2005*, Budapest, Hungary.

Cremer, L. and Müller, H. A. (1978). *Principles and Applications of Room Acoustics*, volume 1. Applied Science Publishers LTD., Barking, Essex, UK.

Funkhouser, T., Tsingos, N., Carlbom, I., Elko, G., Sondhi, M., West, J. E., Pingali, G., Min, P., and Ngan, A. (2004). A beam tracing method for interactive architectural acoustics. *Journal of the Acoustical Society of America*, 115(2):739–756.

Hecht, E. (2002). *Optics*. Pearson Education Inc., San Francisco, CA. USA, 4 edition.

Jensen, H. W. (2001). *Realistic Image Synthesis Using Photon Mapping*. A. K. Peters, Natick, MA. USA.

Kapralos, B., Jenkin, M., and Milios, E. (2005). Acoustical modeling using a Russian roulette strategy. In *Proceedings of the 118th Convention of the Audio Engineering Society*, Barcelona, Spain.

Keller, J. B. (1962). Geometrical theory of diffraction. *Journal of the Optical Society of America*, 52(2):116–130.

Krokstad, A., Strom, S., and Sorsdal, S. (1968). Calculating the acoustical room response by the use of a ray tracing technique. *Journal of Sound and Vibration*, 8(1):118–125.

Kulowski, A. (1985). Algorithmic representation of the ray tracing technique. *Applied Acoustics*, 18(6):449–469.

Tsingos, N., Carlbom, I., Elko, G., Funkhouser, T., and Kubli, B. (2002). Validation of acoustical simulations in the "Bell Labs Box". *IEEE Computer Graphics and Applications*, 22(4):28–37.

Tsingos, N. and Gascuel, J. (1998). Fast rendering of sound occlusion and diffraction effects for virtual acoustic environments. In *Proc. 104th Convention of the Audio Engineering Society*, pages 1–14, Amsterdam, The Netherlands.